Slow-down of Circumpolar Deepwater flow during the Late Neogene: Evidence from a mudwave field at the Argentine continental slope

Gruetzner, J.[1], Uenzelmann-Neben, G.[1], Franke, D.[2], Arndt, J.E.[1]

[1] Alfred-Wegener-Institut, Helmholtz-Zentrum für Polar- und Meeresforschung, Am Alten Hafen 26, D-27568 Bremerhaven, Germany. (Jens.Gruetzner@awi.de, Gabriele.Uenzelmann-Neben@awi.de, Jan.Erik.Arndt@awi.de)

[2] Bundesanstalt für Geowissenschaften und Rohstoffe, Stilleweg 2, D-30655 Hannover, Germany. (Dieter.Franke@bgr.de)

Abstract

Geochemical evidence from boreholes suggests enhanced transport of Northern Component Water (NCW) to southern latitudes from about 6 Ma onwards. However, information on how this change in transport influenced the intensity and position of current systems is sparse. Here we use seismic reflection profiles interpreted together with bathymetric data to investigate current derived deposits at the central Argentine Margin. Upslope migrating mudwaves overlying a late Miocene erosional unconformity provide evidence that Circumpolar Deepwater (CDW) flow slowed down with the onset of NCW inflow. During the last ~3 Ma changes in dimensions and migration rates of the waves are small indicating continuous bottom current flow conditions similar to today with only minor variations in flow speed, suggesting that the Deep Western Boundary Current (DWBC) in the western south Atlantic as observed today, has been a pervasive feature of the global thermohaline circulation system during the Plio-/Pleistocene.

Introduction

During the late Neogene the Earth underwent a cooling trend interrupted only by a subtle warming in the early Pliocene [*Zachos et al.*, 2001]. Changes in deep hydrography associated with these transitions have been reconstructed from interbasinal carbon isotope ($\delta^{13}C$) gradients [*Billups*, 2002; *Hodell and Venz-Curtis*, 2006; *Poore et al.*, 2006] and Neodymium isotopes [*Klevenz et al.*, 2008] measured on sediments. A robust result of these reconstructions is a major change at ~7-6 Ma indicating that nutrient-depleted Northern Component Water (NCW) reached the southern hemisphere possibly due to the subsidence of the Greenland Scotland Ridge (GSR) [*Poore et al.*, 2006; *Wright and Miller*, 1996] and/or the closure of the Panamanian Gateway [*Billups*, 2002; *Haug and Tiedemann*, 1998]. Following this event the relative proportion of NCW (%NCW) in the Southern Ocean was always similar to or even exceeded the present day value. Further steps in $\delta^{13}C$ accompanied by variations in %NCW occur at 2.8 and 1.6 Ma and were associated with the intensification of Northern Hemisphere glaciations and a strong reduction in CDW ventilation during glacial intervals [*Hodell and Venz-Curtis*, 2006].

The sensitivity in the deep ocean chemistry South Atlantic to fluctuations in %NCW is high. Unfortunately drill cores providing continuous sediment records are sparse in this area: Such records are particularly missing for the Argentine basin, a key area in global ocean circulation where surface, intermediate and deep waters of southern origin are introduced into the thermohaline cycle via a contour-following DWBC [*Smythe-Wright and Boswell*, 1998]

We here examine current derived deposits at the Argentine Margin, where a variety of morphological features are diagnostic for along-slope sediment redistribution by the DWBC [*Gruetzner et al.*, 2011; *Gruetzner et al.*, 2012; *Hernández-Molina et al.*, 2009; *Hernández-Molina et al.*, 2010; *Krastel et al.*, 2011; *Preu et al.*, 2012]. In particular the location, orientation and internal structure of a newly detected field of sediment waves (here called mudwaves) at the middle slope allows insights into past variations in long-term bottom flow activity from late Miocene to recent times.

Oceanographic setting

Surface and intermediate circulation encompasses the Brazil-Malvinas Confluence (BMC), where the Falkland/Malvinas Current and the Brazil Current collide and mix (Fig. 1). The confluence axis where both currents are deflected southward is located at 38-39°S on average but seasonal variability of the BMC influences an area between 25°S and 45°S [*Piola and Matano*, 2001].

In water depths of 1000-3500 m the DWBC consists of two CDW fractions: Upper Circumpolar Deep Water (UCDW) and Lower Circumpolar Deep Water (LCDW; Fig. 1)[*Arhan et al.*, 2002]. North of the BMC these two CDW fractions flow above (UCDW) and below (LCDW) poleward directed NCW, which is formed in the high latitudes of the Northern Hemisphere [*Piola and Matano*, 2001]. The interfaces between these water masses as determined by density changes are at ~2000 m (UCDW/NCW) and at ~3500 m (NCW/LCDW) but slightly deepen northward and are vertically displaced by eddies. South of the BMC, today the NCW flows southward somewhat detached from the slope [*Memery et al.*, 2000]. At abyssal depths below 4000 m Antarctic Bottom Water (AABW) flows northward in the DWBC and enters the Brazil Basin through the Vema and Hunter channels [*Hogg et al.*, 1999].

Methods

We interpreted 29 (7150 km) multi-channel seismic lines gathered by the Federal Institute for Geosciences and Natural Resources (BGR) during two surveys (BGR87 and BGR98) using the seismic vessels S.V. Explora and Akademik Lazarev, respectively. The source volume ranged from 4258 in^3 (69.8 l, BGR98) to 4906 in^3 (80.4 l, BGR87), with towed airgun arrays operating at a pressure of 2000 psi. All the seismic data were acquired with a shot point interval of 50 m and a sampling rate of 4 ms. The streamer length during the BGR87 and BGR98 cruises varied from 3000 to 4500 m, with 60 and 240 channels, respectively. Details about the seismic processing can be found in *Franke et al.* [2010] and; *Hinz et al.*,[1999]. We here use the seismostratigraphic model of [*Gruetzner et al.*, 2012]. Swath bathymetry data (HYDROSWEEP DS) from three cruises with R/V Meteor (M29/1, M46/3, M49/2 [*Bleil et al.*, 2001; *Segl* et al., 1994; *Spieß et al.*, 2002]) were jointly edited with the software package QPS Fledermaus.

Observations

All investigated seismic profiles show the presence of sediment waves in the youngest unit at the continental slope (Fig. 2, Fig. S1). Waveshapes are well developed and regular between 42 and 43.5°S (Fig. 2b), while south of 43.5°S more irregular forms with variable heights occur (Fig. 2d). The waves have spacings of 1.5 to 4 km and are 30 to 100 m high. Regular waves show continuous curved internal reflectors converging smoothly towards the seaward wave flanks (Fig. 2b). In contrast irregular waves often show abrupt termination of the reflectors at both wave flanks (Fig. 2d). North of 43.5°S wave crests strike SSW-NNE at ~28° while south of 43.5°S strike angles of 32-38° are observed (Fig. 2a,c). In the majority of cases the wave profiles reveal an asymmetric morphology with a steeper western (upslope) flank but shallower and smoother eastern (downslope) flank. Slight thickening of the upslope flanks can be observed suggesting accretion on that side while at the downslope flanks less deposition or erosion occurs (Fig. 2). As a result the sediment waves migrate upslope in a WNW direction. The migrating sediment waves form an extensive field at a water depth of 2500 to 3500 m (Fig. 3) which is ~75 km wide and can be traced for 350 km within the working area resulting in an area of > 26000 km^2. The southward extension of the field is not known since we do not have access to profiles to the south of the working area. However, sediment waves can also be found within the same water depth range at 47.5°S to 48°S (Fig. S1). A number of submarine canyons can be mapped that dissect the wave field in various places (Fig. 3).

North of 43.5°S seismic section show buried waves directly overlying a strong seismic reflector (Fig 2b). This late Miocene reflector (AR7 of [*Gruetzner et al.*, 2012]), which can be traced throughout the working area, is discontinuous in some places on the upper slope where canyons are intersecting but in the area of the wave field it is continuous. The thickness of the wave field overlying AR7 is 550 – 1100 ms TWT (~600 to 900 m) with decreasing values towards the North.

Another unconformity occurring at ~400 to 500 ms TWT below the sea floor (Fig. 2) in most profiles subdivides the overlying unit and pinches out seaward at ~ 3.8 - 4.0 s TWT. The local reflector, here called P, marks a change in depositional character with more regular mudwaves developing above the unconformity.

Seaward of the wave field a plastered drift with a thickness of ~400 - 600 m and a width of ~10 - 20 km can be traced for ~100 km within the working area [*Gruetzner et al.*, 2012]. The drift is also partly covered with sediment waves and terminates at about 43.5°S where it is replaced northward by another wave field in a water depth range of 4000 to 5000 m (Figs. 3 and S1).

Mudwave migration and bottom current flow

Sedimentary waves are undulating depositional sedimentary structures that develop in various environments where bottom flow patterns are stable over long periods of time [e.g. *Wynn et al.*, 2000]. Wave dimensions and locations indicate that the wave field described here could be either of bottom current origin (mudwaves) or developed under turbidity currents [*Wynn and Stow,* 2002]. The shape of the field does not align with the downslope pathways of major canyons (Fig. 3). Instead it is restricted to a margin parallel area in 2500 to 3500 m water depth. Waves occurring on landward levees of major canyons here migrate away (upslope) from the canyon trough (Fig. S1), which is opposite to what is reported for levees formed by turbidity current overflow [*Carter et al.*, 1990]. Also, a decrease in the rate of wave growth over time is not observed. Such a decrease was found for sediment waves bordering deepening channels with an increasing number of turbidites confined to the channel [*Carter et al.*, 1990]. Furthermore, the sediment waves occur in the vicinity of a contourite drift (Fig. 3) and are also observed in the same water depth range on bottom current shaped slope terraces in the southern Argentine Basin (Fig. S1) [*Gruetzner et al.*, 2011; *Hernández-Molina et al.*, 2009]. Sediment cores obtained within the mudwave area are mud/silt dominated [*Frenz et al.*, 2004] with occasional sand layers. Physical property changes within these sediments were attributed to climatic cycles and don't show comb type patterns with many sharp spikes as typical for frequent distal turbiditic layers [*Segl* et al., 1994]. Based on these observations we conclude that the reported wave field was mainly shaped by bottom currents and that turbidity current influence was only sporadic.

In the central Argentine basin mudwaves are widespread at the Zapiola Drift, and the waves described here may be regarded as the mid-depth counterpart to large wave fields generated by the AABW in depth > 4500 m [e.g. [*Flood et al.*, 1993; *von Lom-Keil et al.*, 2002]. But other than in the deep basin where mudwaves have been in existence since the Late Oligocene [*Manley and Flood*, 1993], reflector AR7 gives good indication that wave growth at the continental slope took place during Plio-Pleistocene.

Modeling studies [*Blumsack and Weatherly*, 1989] as well as empirical investigations on mudwave fields [*Flood et al.*, 1993] suggest that, in the Southern Hemisphere, wave migration should be commonly to the left of the flow direction. The observed upslope wave migration in WNW direction at the Argentine slope is thus in agreement with a north setting bottom current flow during the Plio-Pleistocene. Our results suggest a systematic change in mudwave orientation at ~43.5°S. Northward mudwaves align anti-clockwise (~6°) relative to the regional contours (Fig. 2a) while further south wave crests strike up to ~20° clockwise from the regional contours (Fig. 2c). It is difficult to infer current flow directions from the strike of mud waves [Manley and Caress, 1994], especially when the waves are aligned nearly parallel to the contours (a proxy for current direction) [*Flood et al.*, 1993]. However, for the regular waves north of~43.5°S theoretical models [*Flood*, 1988; *Hopfauf et al.*, 2001] predict an upcurrent wave migration for a wide range (6 to 17 cm/s) of current velocities.

Paleoceanographic implications

The high amplitude seismic marker horizon AR7 was also identified in other studies within the central Argentine margin and adjacent areas [*Cavallotto et al.*, 2011; *Ewing and Lonardi*, 1971; *Schümann*, 2002; *Violante et al.*, 2010]. Based on a correlation with industry well "Cruz del Sur" [*Bushnell et al.*, 2000] AR7 represents an unconformity close to the Miocene/Pliocene boundary [*Schümann*, 2002]. Well "LAPA X-1" in the western Malvinas basin [*Galeazzi*, 1998] and at DSDP Site 512 on the Maurice Ewing Bank [*Ciesielski and Weaver*, 1983] show unconformities of approximately the same age. Furthermore, prominent hiatuses are observed on the intermediate-depth Maurice Ewing Bank (MEB) located at the eastern edge of the Falkland (Malvinas) Plateau with the major phase of erosion occurring between 7.2 and 6.2 Ma (Fig. 4) [*Ciesielski et al.*, 1982], a time of widespread hiatuses in the world oceans [*Barron and Keller*, 1982] affecting also the paleo-depth range between 2000 and 3500 m in the Atlantic [*Keller and Barron*, 1987]. At this time %NCW in the south Atlantic was at a minimum [*Billups*, 2002; *Poore et al.*, 2006] possibly caused by a higher sill depth of the GSR and a deep Panamanian gateway (Fig. 4). This implies that reflector AR7 represents the top of an erosional episode at the central Argentine margin which was caused by vigorous bottom current circulation prior to the increase of NCW transport to the Southern Ocean.

In the majority of the investigated reflection profiles north of 43.5°S buried sediment waves of irregular shape directly overlie reflector AR7 which indicates that current velocities shortly after ~ 6 Ma slowed down into a range where wave growth was possible at the slope. This change correlates with a rapid increase in NCW production [*Poore et al.*, 2006] and a sustained interval of high (three times the present day value) %NCW in the southern ocean [*Billups*, 2002].

Unconformity P indicating a re-accelerated flow cannot be dated via direct borehole correlation in the working area but may correlate to reflector "a", a major regional unconformity in the Weddell and Scotia Sea which was tentatively dated near the Early to Late Pliocene boundary [*Maldonado et al.*, 2006]. Enhanced CDW flow at this time is also indicated by limited deposition and widespread erosion and/or non-deposition over most of the Maurice Ewing Bank from 4.0 to 3.2 Ma [*Ciesielski et al.*, 1982], a time, when %NCW at ODP Site 1088 was at a local minimum [*Billups*, 2002] (Fig. 4).

North of 43.5°S regular waves indicate a stable CDW flow over the last ~3 Ma. Utilizing a lee wave model [*Flood*, 1988] with the observed wave dimensions and the ratio of downstream/upstream flank sedimentation rate (SRR) flow speeds estimated for 10 of these regular waves yield current velocities of 7 to 17 cm/s which on average is slightly higher than a current meter record from the slope (1970 m waterdepth) at ~38.5°S [*Weatherly*, 1993]. A faster northward flow is indicated for the area south of 43.5°S by erosional features like scours and moats. Thus the more regular waves occurring north of 43.5°S may point towards a systematic northward decrease in speed of bottom water masses as noted on a larger scale by [*Hernández-Molina et al.*, 2009] which may be due to the northward increasing interaction of CDW with NCW.

Conclusions

A field of migrating mudwaves at 2500 – 3500 m water depth at the Argentine margin that is described here for the first time and erosional unconformities allow inference of changes in current intensity of CDW from the late Miocene (6 Ma) onward. Slow-downs of the CDW towards moderate flow speeds as indicated by wave growth and migration are found for time intervals with higher NCW inflow into the South Atlantic. In contrast, higher current velocities causing hiatuses are associated with minima in %NCW. Differences in wave shapes and orientations south and north of 43.5°S likely indicate stronger NCW influence towards the North.

Acknowledgement

This research was funded by the Priority Program SAMPLE (South Atlantic Margin Processes and Links with onshore Evolution) of the Deutsche Forschungsgemeinschaft (DFG) under contract no. Ue 49/11 and Ue 49/15. We thank the anonymous reviewers and editor Meric Srokosz for their helpful comments.

References

Arhan, M., X. Carton, A. Piola, and W. Zenk (2002), Deep lenses of circumpolar water in the Argentine Basin, *J. Geophys. Res.*, *107*(C1), 3007, doi: 10.1029/2001JC000963.

Barron, J. A., and G. Keller (1982), Widespread Miocene deep-sea hiatuses - coincidence with periods of global cooling, *Geology*, *10*(11), 577-581, doi: 10.1130/0091-7613(1982)10<577:WMDHCW>2.0.CO;2.

Billups, K. (2002), Late Miocene through early Pliocene deep water circulation and climate change viewed from the sub-Antarctic South Atlantic, *Palaeogeogr. Palaeoclimatol. Palaeoecol.*, *185*(3-4), 287-307, doi: 10.1016/S0031-0182(02)00340-1.

Bleil, U., and cruise participants (2001), Report and preliminary results of Meteor cruise M 46/3 Montevideo–Mar del Plata, 04.01.-07.02. 2000, *Ber. Fachb. Geowiss. Univ. Bremen, 172.*

Blumsack, S. L., and G. L. Weatherly (1989), Observations of the nearby flow and a model for the growth of mudwaves, *Deep-Sea. Res.*, *36*(9), 1327-1339, doi: 10.1016/0198-0149(89)90086-1.

Bushnell, D. C., J. E. Baldi, F. H. Bettini, H. Franzin, E. Kovaks, R. Marinelli, and G. J. Wartenburg (2000), Petroleum system analysis of the Eastern Colorado Basin, offshore Northern Argentine, in *Petroleum systems of South Atlantic margins*, edited by M. R. Mello, pp. 403-415, AAPG Mem. 73.

Carter, L., R. M. Carter, C. S. Nelson, C. S. Fulthorpe, and H. L. Neil (1990), Evolution of Pliocene to Recent abyssal sediment waves on Bounty Channel levees, New-Zealand, *Mar. Geol.*, *95*(2), 97-109, doi: 10.1016/0025-3227(90)90043-J.

Cavallotto, J. L., R. A. Violante, and F. J. Hernández-Molina (2011), Geological aspects and evolution of the Patagonian continental margin, *Biol. J. Linn. Soc*, *103*(2), 346-362, doi: 10.1111/j.1095-8312.2011.01683.x.

Ciesielski, P. F., M. T. Ledbetter, and B. B. Ellwood (1982), The development of Antarctic glaciation and the Neogene paleoenvironment of the Maurice Ewing Bank, *Mar. Geol.*, *46*(1-2), 1-51, doi: 10.1016/0025-3227(82)90150-5.

Ciesielski, P. F., and F. M. Weaver (1983), Neogene and Quaternary paleoenvironmental history of Deep Sea Drilling Project Leg 71 sediments, Southwest Atlantic Ocean, *Initial Rep. Deep Sea Drill. Proj.*, 71, 461–477, doi:10.2973/dsdp.proc.71.120.1983.

Ewing, M., and A. G. Lonardi (1971), Sediment transport and distribution in the Argentine Basin. 5. Sedimentary structure of the Argentine margin, basin, and related provinces, *Phys. Chem. Earth.*, *8*, 123-251, doi: 10.1016/0079-1946(71)90017-6.

Flood, R. D. (1988), A lee wave model for deep-sea mudwave activity, *Deep-Sea. Res.*, *35*(6), 973-983, doi: 10.1016/0198-0149(88)90071-4.

Flood, R. D., A. N. Shor, and P. L. Manley (1993), Morphology of abyssal mudwaves at Project MUDWAVES sites in the Argentine Basin, *Deep-Sea. Res. Pt. II*, *40*(4-5), 859-888, doi: 10.1016/0967-0645(93)90038-O.

Franke, D., S. Ladage, M. Schnabel, B. Schreckenberger, C. Reichert, K. Hinz, M. Paterlini, J. de Abelleyra, and M. Siciliano (2010), Birth of a volcanic margin off Argentina, South Atlantic, *Geochem. Geophys. Geosyst.*, *11*(2), Q0AB04, doi: 10.1029/2009GC002715.

Frenz, M., R. Höppner, J. B. Stuut, T. Wagner, and R. Henrich (2004), Surface sediment bulk geochemistry and grain-size composition related to the oceanic circulation along the South American continental margin in the Southwest Atlantic, in *The South Atlantic in the Late Quaternary*, edited by G. Wefer, et al., pp. 347-373, Springer.

Galeazzi, J. S. (1998), Structural and stratigraphic evolution of the western Malvinas Basin, Argentina, *Am. Assoc. Pet. Geol. Bull., 82(4), 596–636.*

Gruetzner, J., G. Uenzelmann-Neben, and D. Franke (2011), Variations in bottom water activity at the southern Argentine margin: indications from a seismic analysis of a continental slope terrace, *Geo-Mar. Lett.*, *31*(5), 405-417, doi: 10.1007/s00367-011-0252-0.

Gruetzner, J., G. Uenzelmann-Neben, and D. Franke (2012), Variations in sediment transport at the central Argentine continental margin during the Cenozoic, *Geochem. Geophys. Geosyst.*, *13*, Q10003, doi: 10.1029/2012GC004266

Haug, G. H., and R. Tiedemann (1998), Effect of the formation of the Isthmus of Panama on Atlantic Ocean thermohaline circulation, *Nature*, *393*(6686), 673-676, doi: 10.1038/31447.

Hernández-Molina, F. J., M. Paterlini, R. Violante, P. Marshall, M. de Isasi, L. Somoza, and M. Rebesco (2009), Contourite depositional system on the Argentine Slope: An exceptional record of the influence of Antarctic water masses, *Geology*, *37*(6), 507-510, doi: 10.1130/g25578a.1.

Hernández-Molina, F. J., M. Paterlini, L. Somoza, R. Violante, M. A. Arecco, M. de Isasi, M. Rebesco, G. Uenzelmann-Neben, S. Neben, and P. Marshall (2010), Giant mounded drifts in the Argentine Continental Margin: Origins, and global implications for the history of thermohaline circulation, *Mar. Petrol. Geol.*, *27*(7), 1508-1530, doi: 10.1016/j.marpetgeo.2010.04.003.

Hinz, K., S. Neben, B. Schreckenberger, H. A. Roeser, M. Block, K. G. d. Souza, and H. Meyer (1999), The Argentine continental margin north of 48°S: sedimentary successions, volcanic activity during breakup, *Mar. Petrol. Geol.*, *16*(1), 1-25, doi: 10.1016/S0264-8172(98)00060-9.

Hodell, D. A., and K. A. Venz-Curtis (2006), Late Neogene history of deepwater ventilation in the Southern Ocean, *Geochem. Geophys. Geosyst.*, *7*(9), Q09001, doi: 10.1029/2005GC001211.

Hogg, N. G., G. Siedler, and W. Zenk (1999), Circulation and variability at the southern boundary of the Brazil Basin, *J. Phys. Oceanogr.*, *29*(2), 145-157, doi: 10.1175/1520-0485(1999)029<0145:CAVATS>2.0.CO;2.

Hopfauf, V., V. Spieß, and Fachbereich Geowissenschaften (2001), A three-dimensional theory for the development and migration of deep sea sedimentary waves, *Deep-Sea. Res. Pt. I*, *48*(11), 2497-2519, doi: 10.1016/S0967-0637(01)00026-7.

Keller, G., and J. A. Barron (1987), Paleodepth distribution of Neogene deep-sea hiatuses, *Paleoceanography*, *2*(6), 697-713, doi: 10.1029/PA002i006p00697.

Klevenz, V., D. Vance, D. N. Schmidt, and K. Mezger (2008), Neodymium isotopes in benthic foraminifera: Core-top systematics and a down-core record from the Neogene south Atlantic, *Earth Planet. Sci. Lett.*, *265*(3-4), 571-587, doi: 10.1016/j.epsl.2007.10.053.

Krastel, S., G. Wefer, T. Hanebuth, A. Antobreh, T. Freudenthal, B. Preu, T. Schwenk, M. Strasser, R. Violante, and D. Winkelmann (2011), Sediment dynamics and geohazards off Uruguay and the de la Plata River region (northern Argentina and Uruguay), *Geo-Mar. Lett.*, *31*(4), 271-283, doi: 10.1007/s00367-011-0232-4.

Maldonado, A., F. Bohoyo, J. Galindo-Zaldívar, J. Hernández-Molina, A. Jabaloy, F. Lobo, J. Rodríguez-Fernández, E. Suriñach, and J. Vázquez (2006), Ocean basins near the Scotia–Antarctic plate boundary: Influence of tectonics and paleoceanography on the Cenozoic deposits, *Mar. Geophys. Res.*, *27*(2), 83-107, doi: 10.1007/s11001-006-9003-4.

Manley, P. L., and D. W. Caress (1994), Mudwaves on the Gardar Sediment Drift, NE Atlantic, *Paleoceanography*, *9*(6), 973-988, doi: 10.1029/94PA01755.

Manley, P. L., and R. D. Flood (1993), Paleoflow history determined from mudwave migration - Argentine Basin, *Deep-Sea. Res. Pt. II*, *40*(4-5), 1033-1055, doi: 10.1016/0967-0645(93)90047-Q.

Memery, L., M. Arhan, X. A. Alvarez-Salgado, M. J. Messias, H. Mercier, C. G. Castro, and A. F. Rios (2000), The water masses along the western boundary of the south and equatorial Atlantic, *Prog. Oceanogr.*, *47*(1), 69-98, doi: 10.1016/S0079-6611(00)00032-X.

Piola, A. R., and R. P. Matano (2001), Brazil and Falklands (Malvinas) Currents, in *Encyclopedia of Ocean Sciences*, edited by J. H. Steele, et al., pp. 340-349, Academic Press, London.

Poore, H. R., R. Samworth, N. J. White, S. M. Jones, and I. N. McCave (2006), Neogene overflow of Northern Component Water at the Greenland-Scotland Ridge, *Geochem. Geophys. Geosyst.*, *7*, doi: 10.1029/2005GC001085.

Preu, B., T. Schwenk, F. J. Hernandez-Molina, R. Violante, M. Paterlini, S. Krastel, J. Tomasini, and V. Spieß (2012), Sedimentary growth pattern on the northern Argentine slope: The impact of North Atlantic Deep Water on southern hemisphere slope architecture, *Mar. Geol.*, *329-331*(0), 113-125, doi: 10.1016/j.margeo.2012.09.009.

Schümann, T. K. (2002), The hydrocarbon potential of the deep offshore along the Argentine volcanic rifted margin - a numerical simulation, PhD thesis, 194 pp., RWTH Aachen, Aachen, Germany.

Smythe-Wright, D., and S. Boswell (1998), Abyssal circulation in the Argentine Basin, *J. Geophys. Res.*, *103*(C8), 15845-15851, doi: 10.1029/98JC00142

Segl, M., and cruise participants (1994), Report and preliminary results of Meteor-cruise M 29/1: Buenos-Aires- Montevideo, 17.6. - 13.7.94, *Ber. Fachb. Geowiss. Univ. Bremen*, 94.

Spieß, V., and cruise participants (2002), Report and preliminary results of Meteor Cruise M 49/2, Montevideo (Uruguay)-Montevideo, 13.02.-07.03. 2001, *Ber. Fachb. Geowiss. Univ. Bremen*, 84.

Violante, R. A., C. M. Paterlini, I. P. Costa, F. J. Hernández-Molina, L. M. Segovia, J. L. Cavallotto, S. Marcolini, G. Bozzano, C. Laprida, N. García Chapori, T. Bickert, and V.

Spieß (2010), Sismoestratigrafia y evolución geomorfológica del talud continental adyacente al litoral del este bonaerense, Argentina, *Latin American journal of sedimentology and basin analysis*, *17*(1), 33-62.

von Lom-Keil, H., V. Spieß, and V. Hopfauf (2002), Fine-grained sediment waves on the western flank of the Zapiola Drift, Argentine Basin: evidence for variations in Late Quaternary bottom flow activity, *Mar. Geol.*, *192*(1-3), 239-258, doi: 10.1016/S0025-3227(02)00557-1.

Weatherly, G. L. (1993), On deep-current and hydrographic observations from a mudwave region and elsewhere in the Argentine Basin, *Deep-Sea. Res. Pt. II*, *40*(4-5), 939-961, doi: 10.1016/0967-0645(93)90042-L.

Wright, J. D., and K. G. Miller (1996), Control of North Atlantic Deep Water circulation by the Greenland-Scotland Ridge, *Paleoceanography*, *11*(2), 157-170, doi: 10.1029/95PA03696.

Wynn, R. B., P. P. E. Weaver, G. Ercilla, D. A. V. Stow, and D. G. Masson (2000), Sedimentary processes in the Selvage sediment-wave field, NE Atlantic: new insights into the formation of sediment waves by turbidity currents, *Sedimentology*, *47*(6), 1181-1197, doi: 10.1046/j.1365-3091.2000.00348.x.

Wynn, R. B., and D. A. V. Stow (2002), Classification and characterisation of deep-water sediment waves, *Mar. Geol.*, *192*(1-3), 7-22, doi: 10.1016/S0025-3227(02)00547-9.

Zachos, J., M. Pagani, L. Sloan, E. Thomas, and K. Billups (2001), Trends, rhythms, and aberrations in global climate 65 Ma to present, *Science*, *292*(5517), 686-693, doi: 10.1126/science.1059412.

Figure captions

Figure 1. Study area with locations of seismic profiles and swath bathymetry. Inset shows generalized present day oceanographic situation: AAIW = Antarctic Intermediate Water, AABW = Antarctic Bottom Water; CDW = Circumpolar Deep Water and NCW = Northern Component Water, MC = Malvinas Current, BC = Brazil Current, BMC = Brazil-Malvinas Confluence. Black dot marks position of well “Cruz del Sur”.

Figure 2. Bathymetric and seismic images of mudwaves north (a, b) and south (c, d) of 43.5°S. Arrows in a and c indicate directions of regional contours, mudwave alignment and wave migration.

Figure 3. Bathymetric chart with location of mudwave fields and a contourite drift at the Argentine margin. Arrows indicate bottom water flow: AABW = Antarctic Bottom Water; CDW = Circumpolar Deep Water, NCW = Northern Component Water. Canyons are shown in red. Contouritic channels are shown in orange.

Figure 4. Evolution of erosional unconformities and mudwaves (right) in comparison to occurrences of major hiatuses at the Maurice Ewing bank (center) [*Ciesielski et al.*, 1982] and %NCW in the south Atlantic (left) [*Billups*, 2002].

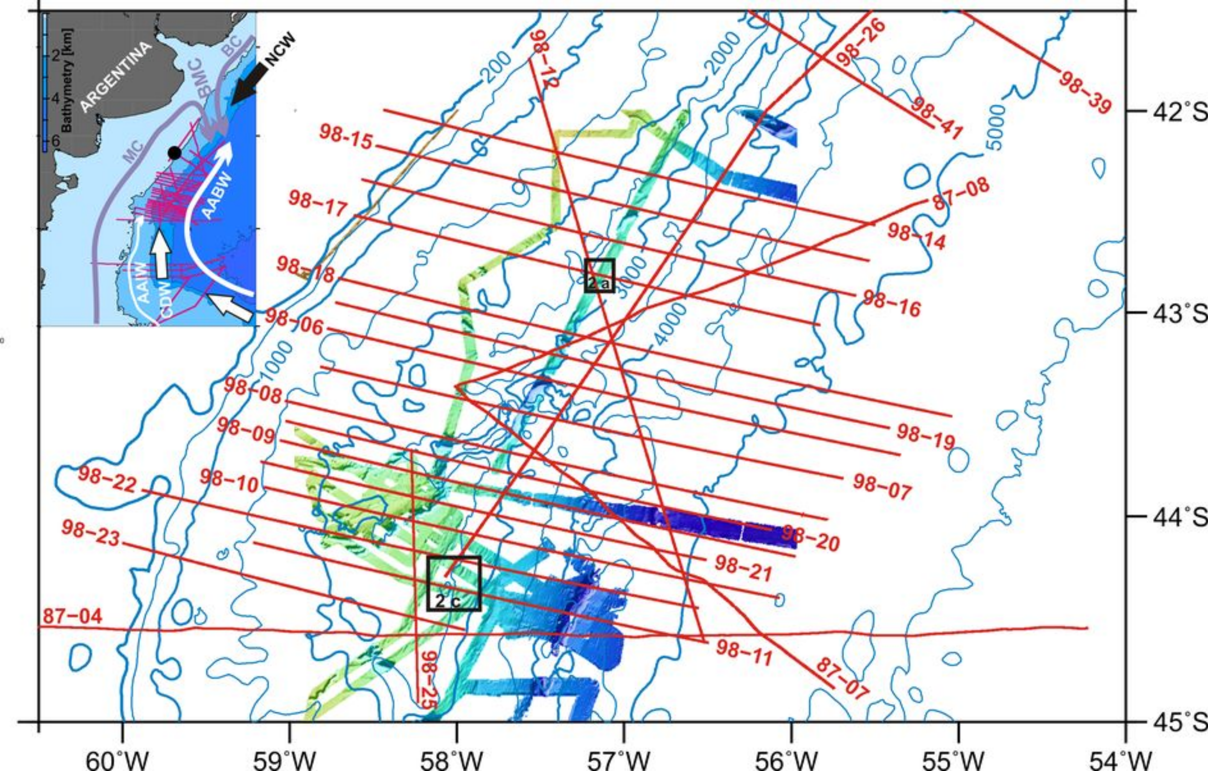
Bathymetry [km]
2
4
6
ARGENTINA
BC
BMC
MC
NCW
AABW
AAIW
CDW
200
1000
2000
3000
4000
5000
98-26
98-12
98-39
98-41
98-15
98-17
87-08
98-14
98-18
2 a
98-16
98-06
98-08
98-19
98-09
98-07
98-22
98-10
98-20
98-23
98-21
2 c
87-04
98-11
98-25
87-07
42°S
43°S
44°S
45°S
60°W
59°W
58°W
57°W
56°W
55°W
54°W

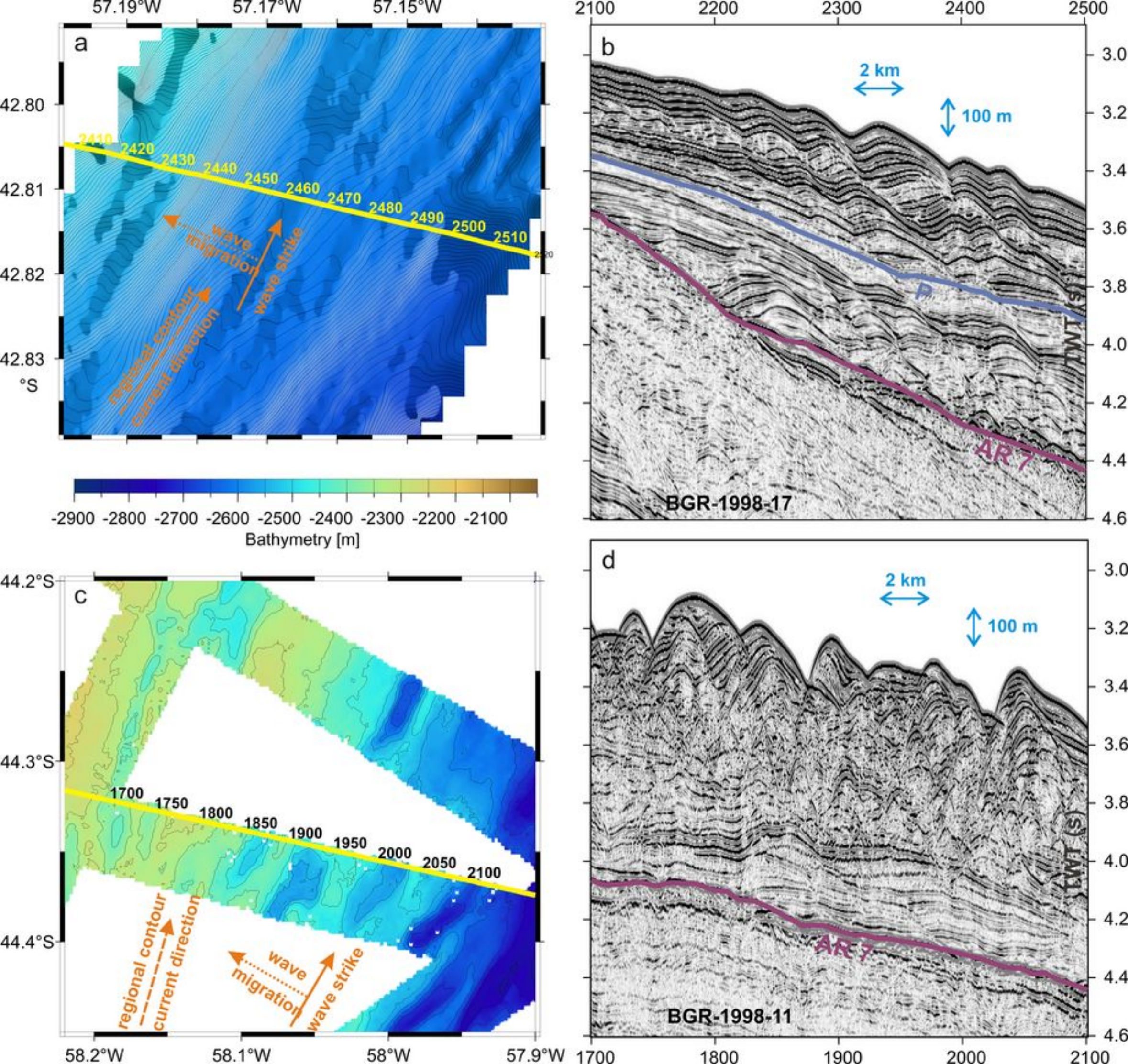

a
57.19°W
57.17°W
57.15°W
42.80
42.81
42.82
42.83
°S
2410
2420
2430
2440
2450
2460
2470
2480
2490
2500
2510
wave
migration
wave strike
regional contour
current direction
-2900
-2800
-2700
-2600
-2500
-2400
-2300
-2200
-2100
Bathymetry [m]
b
2100
2200
2300
2400
2500
2 km
100 m
P
AR 7
BGR-1998-17
TWT (s)
3.0
3.2
3.4
3.6
3.8
4.0
4.2
4.4
4.6
c
44.2°S
44.3°S
44.4°S
1700
1750
1800
1850
1900
1950
2000
2050
2100
regional contour
current direction
wave
migration
wave strike
58.2°W
58.1°W
58°W
57.9°W
d
1700
1800
1900
2000
2100
2 km
100 m
AR 7
BGR-1998-11
TWT (s)

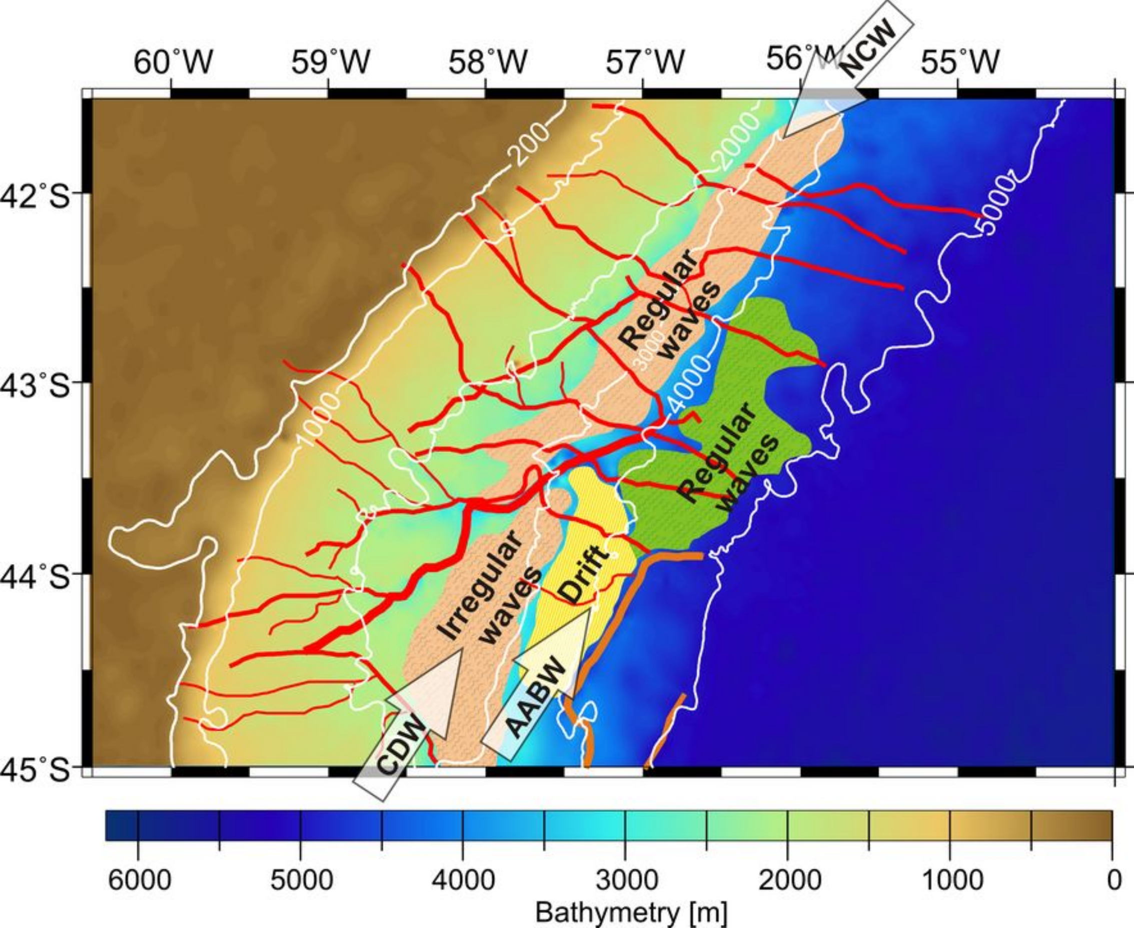

60°W
59°W
58°W
57°W
56°W
55°W
42°S
43°S
44°S
45°S
NCW
CDW
AABW
Regular waves
Regular waves
Irregular waves
Drift
200
1000
2000
3000
4000
5000
6000
5000
4000
3000
2000
1000
0
Bathymetry [m]

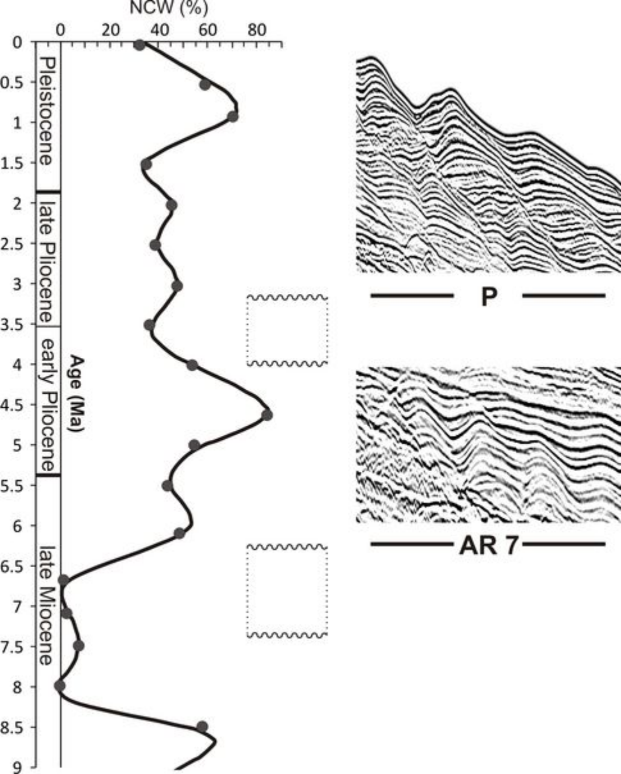
NCW (%)
0
20
40
60
80
0
0.5
1
1.5
2
2.5
3
3.5
4
4.5
5
5.5
6
6.5
7
7.5
8
8.5
9
Pleistocene
late Pliocene
early Pliocene
late Miocene
Age (Ma)
P
AR 7